4. A. C. Grandison, *Bull. Br. Mus. (Nat. Hist.) Zool.* **39**, 299 (1980); I. Griffiths, *Proc. Zool. Soc. London* **132**, 457 (1959); J. D. Lynch and P. M. Ruiz-Carranza, *Proc. Biol. Soc. Wash.* **95**, 557 (1982); L. Trueb and P. Alberch, in *Functional Morphology of Vertebrates*, H. R. Duncker and G. Fleischer, Eds. (Fisher, Stuttgart, in press).
5. R. L. Carroll and R. Holmes, *Zool. J. Linn. Soc.* **68**, 1 (1980).
6. J. Hanken, *J. Morphol.* **174**, 57 (1982).
7. _____, *ibid.* **177**, 255 (1983); *Biol. J. Linn. Soc.* **23**, 55 (1984).
8. R. L. Carroll, *Biol. Rev. (Cambridge)* **44**, 393 (1969).
9. O. Rieppel, *J. Zool. London* **204**, 289 (1984); K. Forsgaard, in *Advances in Herpetology and Evolutionary Biology*, A. G. J. Rhodin and K. Miyata, Eds. (Museum of Comparative Zoology, Harvard University, Cambridge, Mass., 1983), pp. 284–295.
10. O. Rieppel, *Symp. Zool. Soc. London* **52**, 503 (1984).
11. C. Gans, *Bull. Am. Mus. Nat. Hist.* **119**, 129 (1960).
12. D. B. Wake, *Mem. South. Calif. Acad. Sci.* **4**, 1 (1966).
13. _____ and J. F. Lynch, *Sci. Bull. Nat. Hist. Mus. Los Angeles Cty.* **25**, 1 (1976).
14. D. Wake and P. Elias, *Contrib. Sci. Nat. Hist. Mus. Los Angeles Cty.* **345**, 1 (1983).
15. J. Hanken, *Copeia* **1983**, 1051 (1983).
16. P. Elias and D. B. Wake, in *Advances in Herpetology and Evolutionary Biology*, A. G. J. Rhodin and K. Miyata, Eds. (Museum of Comparative Zoology, Harvard University, Cambridge, Mass., 1983), pp. 1–12.
17. Specimens were prepared as cleared whole mounts differentially stained for bone and cartilage (*6*). Specimens examined of most species are listed in J. Hanken, *Morphological and Genetic Investigations of Miniaturization in Salamanders (Genus* Thorius*)* (University Microfilms, Ann Arbor, Mich., 1980). Additional specimens are as follows: *Thorius* sp. A, M (Mexican field tag series) 5541-5542, and *Thorius* sp. E, M 5097-5098, HBS (H. B. Shaffer field tag series) 2257, 2259. Specimens are deposited in the Museum of Vertebrate Zoology, University of California, Berkeley. Data are unavailable for the extremely rare terrestrial species *Thorius dubitus*.
18. The fusion combinations are as follows: 1, ulnare, intermedium; 2, ulnare, intermedium, centrale; 3, distal carpal 4, centrale; 4, distal carpal 3, distal carpal 4, centrale; 5, distal carpal 1-2, distal carpal 3, distal carpal 4, centrale; 6, distal carpal 1-2, centrale; 7, radiale, centrale 1; 8, distal carpal 1-2, distal carpal 3; and 9, distal carpal 3, distal carpal 4.
19. A. Larson, *Evolution* **37**, 1141 (1983); P. Alberch, *ibid.*, p. 906.
20. J. F. Lynch and D. B. Wake, *Contrib. Sci. Nat. Hist. Mus. Los Angeles Cty.* **294**, 1 (1978).
21. P. Alberch, *Evolution* **35**, 84 (1981).
22. The primitive plethodontid arrangement is ulnare, intermedium, radiale, centrale, centrale 1, and distal carpals 1-2, 3, and 4 (*12*).
23. D. B. Wake, in *Evolution Today*, G. G. E. Scudder and J. L. Reveal, Eds. (Hunt Institute for Botanical Documentation, Pittsburgh, 1981), pp. 257–270.
24. Estimates of genetic distance, *D* [M. Nei, *Am. Nat.* **106**, 283 (1972)], are based on electrophoretic variation of 16 protein loci in 69 populations (mean n = 11.3 specimens) from 55 localities and including all known valid species (*15*). Conspecific populations from the original unweighted pair-group method analysis dendrogram [P. H. A. Sneath and R. R. Sokal, *Numerical Taxonomy* (Freeman, San Francisco, 1973)] were combined to yield a single terminal branch.
25. A. Larson *et al.*, *Evolution* **35**, 405 (1981); D. B. Wake, *Am. Zool.* **20**, 756 (1980).
26. R. E. Lombard, in *Contributions to Vertebrate Evolution 2*, M. K. Hecht and F. S. Szalay, Eds. (Karger, Basel, 1977), pp. 1–143; R. E. Lombard and D. B. Wake, *J. Morphol.* **153**, 39 (1977); G. Roth *et al.*, *Arch. Biol. Med. Exp.* **16**, 329 (1983).
27. I thank A. Larson, N. Staub, D. Norris, and S. Susnowitz for suggestions on earlier drafts. Supported by the Museum of Vertebrate Zoology, the Center for Latin American Studies, and Sigma Xi, University of California, Berkeley; the Council on Research and Creative Work and NIH grant 1 R23 DE07190-01, University of Colorado, Boulder.

25 February 1985; accepted 12 July 1985

Relation of Spectral Types to Oil Droplets in Cones of Turtle Retina

Abstract. *The spectral sensitivities and color of oil droplets of cone photoreceptors in the retina of the red-eared turtle* (Pseudemys scripta elegans) *were investigated by intracellular recording and injections of Lucifer yellow dye. Six morphological types of cones could be distinguished by the color of the oil droplets located in the outermost inner segments. Single cones containing either red or pale green oil droplets were sensitive to red light, cones with yellow oil droplets to green, and cones with clear oil droplets to blue. Contrary to previous reports, both principal and accessory members of double cones were sensitive to red, and no diffusion of dye was detected between the two apposed members. Thus, the oil droplets provide a reliable morphological basis for further investigation of the neuroanatomical networks underlying the processing of color information in the vertebrate retina.*

TERUYA OHTSUKA
Department of Information Physiology, National Institute for Physiological Sciences, Okazaki 444, Japan

Cone photoreceptors in the turtle retina have characteristic morphological organelles, that is, colored oil droplets. In the red-eared turtle, absorption spectra of the visual pigments measured by microspectrophotometry (MSP) (*1*) were correlated with the color of oil droplets: cones with either red or orange (principal member of double cones) oil droplets contained a red-absorbing visual pigment, cones with yellow oil droplets and the accessory member of double cones contained a green-absorbing visual pigment, and cones with colorless oil droplets contained a blue-absorbing visual pigment. These three distinct spectral types of cones were confirmed by intracellular recordings (*2, 3*). Thus, the oil droplets were used to identify the spectral types of cones in anatomical studies (*4–7*). A recent MSP study (*8*), however, has called into question data on the oil droplet–visual pigment combinations in the red-eared turtle. Intracellular stainings with Lucifer yellow (*9*) has shown that two-thirds of the cones with colorless oil droplets were actually red-sensitive. In addition, the accessory members of double cones in Reeves' turtle were not green-sensitive (*10*), as would be expected from earlier reports. Because color information processing in the vertebrate retina has frequently been studied in red-eared turtles, I have reexamined the question of the color of the oil droplets in the three spectral types of cones. Through the use of intracellular staining with Lucifer yellow, I have confirmed some of the previous oil droplet–spectral sensitivity combinations, but new evidence suggests that some earlier identification (*4–7*) needs to be reevaluated.

Eyecup preparations of the light-adapted red-eared turtle, *Pseudemys scripta elegans*, (carapace length, 18 to 22 cm) were used. Cones located about 2 mm dorsal to the visual streak were investigated. Details of the experimental procedures were as described elsewhere (*10, 11*). A total of 215 cells, whose somata were located at the outer nuclear layer, were recorded from intracellularly and filled with Lucifer yellow CH. About half of the filled cells were excluded by morphological inspection—42 displaced bipolar cells and 50 cones from which the dye had leaked. Thus, definite morphological identification was obtained in 123 cones in which pairing of spectral sensitivity and color of the oil droplet was investigated (Table 1).

In a whole-mounted isolated turtle retina, photoreceptors were of seven morphological types (*4, 9*): rods with no oil droplet and six types of cones containing different colored oil droplets (Fig. 1). Single cones contained either red, pale green (or fluorescent) (*9*), yellow, or clear oil droplets. Double cones were the apposition of two dissimilar cones formed as a figure theta, with the principal member containing an orange oil droplet and the accessory member having none.

Spectral sensitivities (*11*) were obtained from 85 single cones. Sixty cones contained a red oil droplet, the most distinctive type because of the dense red carotinoid (*1*) that absorbed the yellow fluorescence emitted from the Lucifer yellow. A fluorescent ring was seen in the flat-mounted preparation (Fig. 1A). These cones had a peak spectral sensitivity at 620 nm (Fig. 2A). For wavelengths longer than 620 nm, each spectral sensitivity curve agreed with the calculated absorption spectrum of the red-absorbing visual pigment and red oil droplet combination (*12*). Large variations were seen for the shorter wavelengths (<540

nm), which could be explained by assuming that the interposing oil droplet absorbed fewer light stimuli off the axis of the outer segment (*2*). "Colorless" oil droplets can be subdivided into two types, the one tinted pale green and the other appearing clear (*9*). The former is also characterized by its strong autofluorescence (*9*). Six cones containing the pale green oil droplet (Fig. 1B) were red-sensitive. Spectral sensitivities of these cones (Fig. 2B) were higher in the shorter wavelengths than those for most of the cones with red oil droplets, probably because pale green oil droplets absorbed less of the shorter wavelength of the incident light. Sixteen cones containing yellow oil droplets (Fig. 1C) had peak sensitivities at either 540 or 580 nm (Fig. 2C) (*11*). The spectral sensitivity of most of these cones agreed well with the combined absorption spectrum of the green-absorbing pigment and yellow oil droplet (*12*), but each sensitivity curve varied at the shorter wavelengths, as it did for the cones with red oil droplets. Three cones contained the clear oil droplet (Fig. 1D), which was the smallest droplet in the same retinal area (Table 1). Peak spectral sensitivity was at 460 nm (Fig. 2D). An oblique axon (*4*) was found for the cone shown, but the two other cones with clear oil droplets had straight axons.

Table 1. Relation of spectral sensitivities and oil droplets of the cones in the *Pseudemys* retina. λ_{max} refers to maximum sensitivity (*11*), and $\lambda_{1/2}$ is the half-transmission wavelength of oil droplets (*1*). The diameter of oil droplets in the freshly isolated retina was measured in cones located about 2 mm dorsal to the visual streak [mean and (standard deviation), $n = 30$]. Population refers to the number of cones in the same retinal area, where 1 percent is 98 cones per square millimeter. Rods (4 percent) were not listed. Calculated peak is the peak wavelength of the calculated absorption spectra of the visual pigment–oil droplet combinations (*12*).

Spectral type			Oil droplet				Calculated peak (nm)
Sensitivity	λ_{max} (nm)	Cones (*n*)	Color	$\lambda_{1/2}$ (nm)	Diameter (μm)	Population (%)	
Red	620	60	Red	602	8.5 (0.3)	30	640
	620	6	Pale-green		6.1 (0.3)	9	623
	620	19	Orange*	563	7.3 (0.3)	17	626
	620	19	None†			17	623
Green	540	16	Yellow	537	7.1 (0.2)	18	563
Blue	460	3	Clear		5.2 (0.3)	5	462

*Principal member of a double cone. †Accessory member of a double cone.

Since Lucifer yellow was detected only in the one member of a double cone (Fig. 1, E and F), the site of intracellular recording was unequivocally identified in the 38 Lucifer yellow–filled double cones (*13*). In 19 cones, the principal members were impaled (Fig. 1E). The

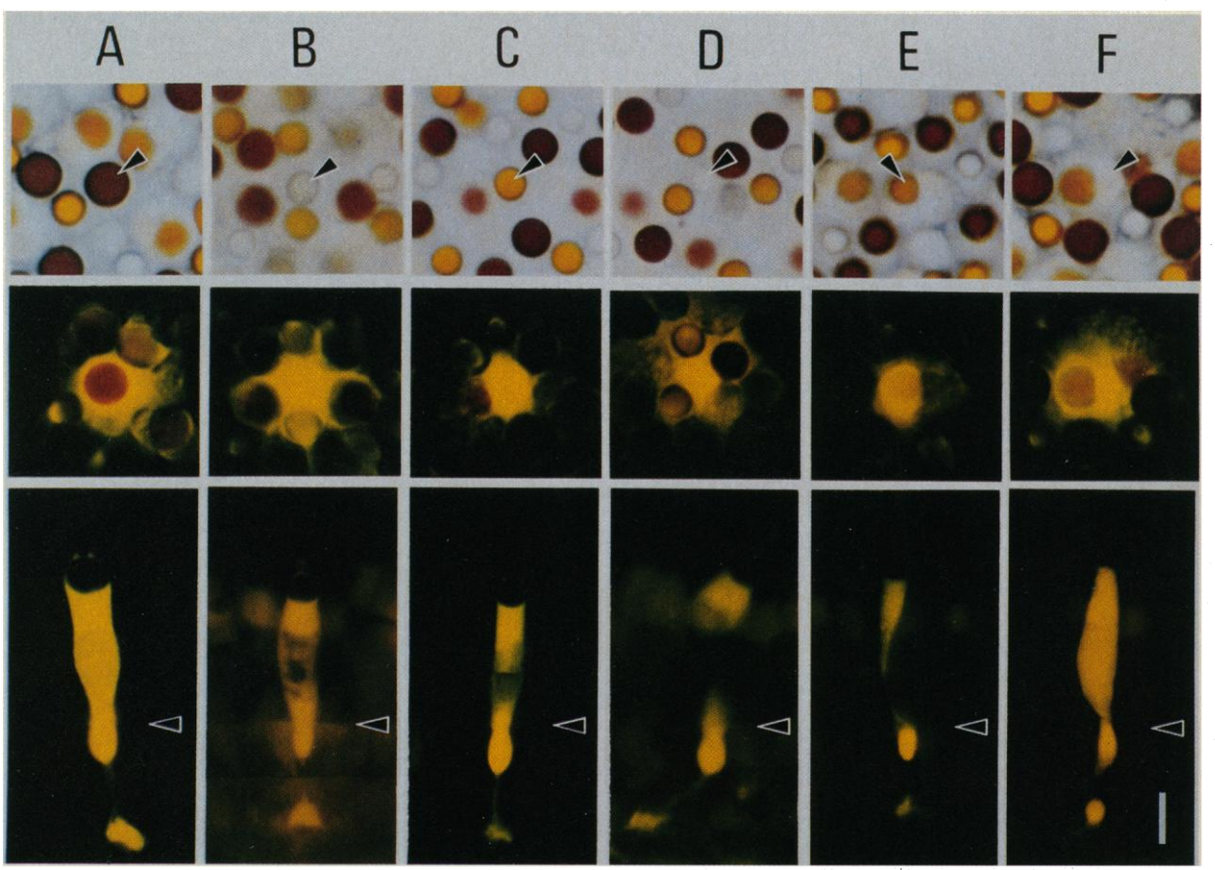

Fig. 1. Photomicrographs of cone photoreceptors filled with Lucifer yellow in the *Pseudemys* retina. Each column displays one of the six morphological types of cone identified by the different colored oil droplets, single cones containing (A) red, (B) pale green, (C) yellow, and (D) clear oil droplets. Double cones consisted of (E) a principal member containing an orange oil droplet and (F) an accessory member with no oil droplet. (Upper row) Light micrographs of the flat-mounted isolated retinas viewed from the photoreceptor side. Arrowheads indicate cones filled with Lucifer yellow. (Middle row) Fluorescent micrographs of identical retinas as used for the upper row. Because the retinal preparations were transparent, the fluorescence of Lucifer yellow was scattered. (Lower row) Fluorescent micrographs of a radial view of each type of cone. Thickness of sections, 10 μm. Some distal inner segments were removed during histological procedures (D). Radial sections of the double cones (E and F) were made perpendicular to the apposed region, and no diffusion of Lucifer yellow was detected between two members. Horizontal arrowheads indicate outer limiting membrane. Magnification is the same throughout; scale bar in (F) is 10 μm.

fluorescence photomicrograph of the whole-mounted preparation delineated a semicircular profile of the inner segment. Details of the inner segment of the principal member were clearly seen in radial section: the principal member appeared as a skewed tube apposing a fat inner segment of the accessory member (the accessory member is shown in Fig. 1F). All principal members were red-sensitive (Fig. 2E). Little filtering effect of the orange oil droplet was seen, perhaps because of non-axial stimuli (*2*).

Although both rods and accessory members had no oil droplets, the paired appearance of double cones could be readily distinguished in the flat-mounted preparation (Fig. 1F). When the dye was injected into the accessory member, no diffusion into the principal member was detected. Radial sections made perpendicular to the apposed region showed only a fat and round inner segment of the accessory member. Spectral sensitivities of 19 accessory members impaled showed a maximum peak at 620 nm (Fig. 2F). MSP studies have yielded conflicting evidence concerning the spectral absorption properties of turtle visual pigment, that is, evidence of either green-absorbing (*1*) or red-absorbing (*8*) pigment. This study supports the latter observation. Furthermore, neither member showed the shift of the peak response from 620 nm as a result of red background illumination (*15*). As no diffusion of the dye was detected between apposed members of double cones, they are probably electrically independent (*16*).

The results confirmed some previous studies (*1*), but earlier conclusions about two types of cones need revision: (i) cones containing pale green oil droplets, which were thought to be blue-sensitive, are actually red-sensitive, and (ii) the accessory members of double cones, which were thought to be green-sensitive (*1, 3*), are also red-sensitive. These results agree well with recent MSP measurements (*8*). Thus, the present results indicate that the anatomical studies based on previous relationships between oil droplet and spectral type of cones should be reevaluated in line with the new data.

The oil droplets, which were the single morphological characteristic that most decidedly identified the three spectral types of cones in the red-eared turtle, should provide a reliable morphological basis for further investigation of neuroanatomical networks in the vertebrate retina.

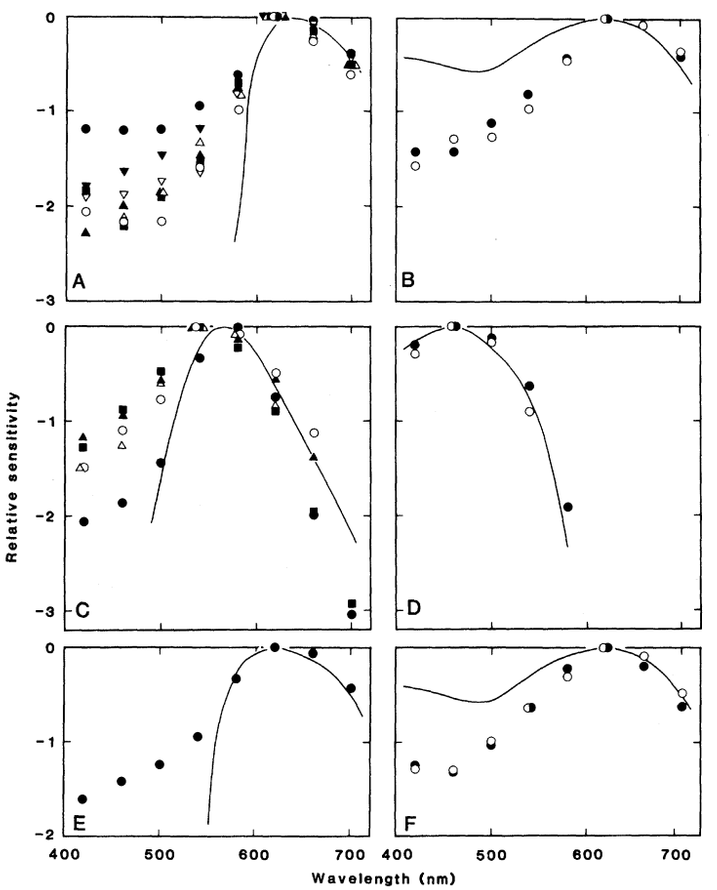

Fig. 2. Spectral sensitivity of six types of cones to test flashes of different wavelength. (A to D) Single cones containing red, pale green, yellow, and clear oil droplets, respectively. (E and F) Principal and accessory members of double cones. Each symbol represents a different cone. Continuous lines (A, C, and E) are the calculated absorption spectra of the visual pigment-oil droplet combinations (*12*). Note the sharp cut-off in the shorter wavelength due to the colored oil droplet. Both pale green and clear oil droplets transmit the visible light, and therefore the absorption spectra of the red- (B and F) and blue-absorbing (D) pigments (*8*) are illustrated by continuous lines.

References and Notes

1. P. A. Liebman, *Handbook of Sensory Physiology*, vol. 7, part 1, *Photochemistry of Vision*, H. J. A. Dartnall, Ed. (Springer-Verlag, Berlin, 1972), p. 507; _____ and A. M. Granda, *Vision Res.* **11**, 105 (1971); *Nature (London)* **253**, 370 (1975).
2. D. A. Baylor and R. Fettiplace, *J. Physiol. (London)* **248**, 433 (1975); D. A. Baylor, M. G. F. Fuortes, P. M. O'Bryan, *ibid.* **214**, 265 (1971); D. A. Baylor and A. L. Hodgkin, *ibid.* **234**, 163 (1973).
3. A. Richter and E. J. Simon, *ibid.* **242**, 673 (1974).
4. H. Kolb and J. Jones, *J. Comp. Neurol.* **209**, 331 (1982).
5. _____, *Proc. Int. Soc. Eye Res.* **2** (Abstr.), 27 (1982).
6. H. F. Leeper, *J. Comp. Neurol.* **182**, 795 (1978).
7. R. A. Normann, I. Perlman, H. Kolb, J. Jones, S. J. Daly, *Science* **224**, 625 (1984).
8. L. E. Lipetz, *The Visual System*, A. Fein, Ed. (Liss, New York, 1985), p. 107; _____ and E. F. MacNichol, Jr., *Biol. Bull.* **163**, 396 (1982).
9. T. Ohtsuka, *Neurosci. Lett.* **52**, 241 (1984).
10. _____, *J. Comp. Neurol.* **237**, 145 (1985).
11. Spectral sensitivity was obtained by the responses to whole-field illumination with monochromatic flashes (duration, 0.3 second) from 420 nm to 700 nm in 40-nm steps. Therefore, the peak wavelength of the spectral sensitivity (Table 1) was the best estimate. Spectral sensitivities of cells shown in Fig. 2 were determined by the standard method of measuring the light intensity producing a criterion amplitude (2 to 5 mV at peak response, which was less than one-third of the saturating amplitude) (*2*). Most of the cone responses, however, were small in amplitude (<5 mV) to saturating light intensities, and the microelectrode was easily dislodged within a few minutes. To collect as many samples as possible, the spectral sensitivities of cells included in Table 1 were obtained by the following simplified procedures. At first, cone responses were recorded to a series of monochromatic flashes at the light intensity that elicited response peak amplitudes less than half of the maximum saturating amplitude. Then the template of intensity-amplitude relation was obtained by stimulating with white light at various intensities. The intensity of white light that elicited a given response amplitude for certain monochromatic stimuli was calculated, and its inverse was considered the sensitivity.
12. The calculated absorption spectra of six types of cones were the products of the absorption spectrum of a cone's visual pigment (*8*) and the transmittance of an oil droplet (*1*). Single cones with a red or a pale green oil droplet and both members of double cones contained the red-absorbing pigment (λ_{max}, 623 nm), cones with a yellow oil droplet the green-absorbing pigment (λ_{max}, 522 nm), and cones with a clear oil droplet the blue-absorbing pigment (λ_{max}, 462 nm) (*8*).
13. A possibility that the gap junction of the double cones (*5*) was somehow blocked in the experimental condition was excluded; the luminosity horizontal cells (*14*) injected with Lucifer yellow in the same eyecup preparation showed a meshwork structure of interwoven axon terminals. Double cones in the ventral retina (*4, 5*) showed no diffusion of Lucifer yellow. Each member was also injected with Procion yellow (*3*), but dye diffusion could not be detected.
14. T. Ohtsuka, *J. Comp. Neurol.* **220**, 191 (1983); M. Piccolino, J. Neyton, P. Witkovsky, H. M. Gerschenfeld, *Proc. Natl. Acad. Sci. U.S.A.* **79**, 3671 (1982).
15. Spectral sensitivities with two peaks to red and green flashes (*3, 7*) were identified as coming from displaced bipolar cells. Most displaced bipolar cells were red-sensitive and showed hy-

perpolarization with no apparent center-surround antagonistic polarization. An electron microscopic study of serial sections revealed that about 30 percent of the retinal cells, whose somata were located in the outer nuclear layer, were displaced bipolar cells (N. Kouyama and T. Ohtsuka, *Brain Res.*, in press).
16. Similar results have also been reported in other vertebrate retinas [D. I. Attwell, F. S. Werblin, M. Wilson, S. M. Wu, *J. Physiol. (London)* **341**, 74P (1983); D. A. Burkhardt, G. Hassin, J. S. Levine, E. F. MacNichol, Jr., *ibid.* **309**, 215 (1980)].
17. I thank A. Kaneko, A. T. Ishida, and R. Siminoff for discussions and comments; L. E. Lipetz for data on visual pigments; W. W. Stewart for the gift of Lucifer yellow CH; and H. Maebashi for technical assistance.

16 November 1984; accepted 23 July 1985

Infection of the Basal Ganglia by a Murine Coronavirus

Abstract. *The coronavirus, mouse hepatitis virus strain A59 (MHV-A59), causes mild encephalitis and chronic demyelination. Immunohistochemical techniques showed that MHV-A59–infected C57BL/6 mice contained dense deposits of viral antigen in the subthalamic nucleus and substantia nigra, with fewer signs of infection in other regions of the brain. The animals showed extra- and intracellular vacuolation, neuronal loss, and gliosis in the subthalamic-nigral region. Such localization is unprecedented among known viral encephalitides of humans and other species. This infection by a member of a viral class capable of causing both encephalitis and persistent infection in several species may be related to postencephalitic parkinsonism.*

PAUL S. FISHMAN*
JENNIFER S. GASS
PEGGY T. SWOVELAND
Department of Neurology and *the Veterans Administration Research Laboratories, University of Maryland School of Medicine, Baltimore 21201*
EHUD LAVI
MAUREEN K. HIGHKIN
SUSAN R. WEISS
Department of Microbiology, University of Pennsylvania School of Medicine and *the Wistar Institute, Philadelphia 19104*

*To whom requests for reprints should be addressed.

Coronaviruses cause encephalitis in several animal species, although in humans they are recognized primarily as respiratory pathogens (*1*, *2*). In mice the A59 strain of mouse hepatitis virus (MHV-A59) causes a chronic demyelinating disease with minimal encephalitis (*3*). MHV-A59 replicates readily in glial cells in vitro but has little propensity to infect neurons (*4*). We wished to further examine the neural tropism of this virus in mice. Using immunohistochemical methods, we observed a strong tropism for the basal ganglia in the region of the subthalamic nucleus and substantia nigra.

Mice of strain C57BL/6 were infected with MHV-A59 (*5*) by intracerebral inoculation at 4 to 6 weeks of age (Table 1). Animals rated as unaffected appeared normal by routine observation. Mice rated as moderately affected showed piloerection and a hunched posture, while those rated as severely affected had marked reduction or difficulty in locomotion, with many appearing moribund. Deaths due to encephalitis or hepatitis usually occurred within 2 weeks of infection. At intervals the animals were killed and perfused with 10 percent buffered formalin or paraformaldehyde-lysine-periodate (PLP) fixative for immunohistochemical and light microscopic examination or with 4 percent buffered glutaraldehyde for ultrastructural examination. To locate viral antigens, we performed immunohistochemical analysis of fixed frozen sections (10 μm) and sections cut from paraffin-embedded material (6 to 8 μm), with comparable results. Antiserum raised in rabbits against detergent-disrupted MHV-A59 was used as the primary antiserum for the peroxidase-antiperoxidase staining technique (*6*), and diaminobenzidine was used as the chromagen.

No significant staining was seen in sections from uninfected control brains with immune antiserum to MHV-A59 or from infected animals incubated with preimmune serum. However, antigen-positive cells were clearly seen in sections from infected animals incubated with the antiserum. The number of immunoreactive cells was closely related to the clinical severity of the encephalitis and the interval between inoculation and death. Viral antigens were present in the brain in greatest amounts within the first 2 weeks after inoculation. In all animals in which sufficient numbers of antigen-positive cells were present for their distribution to be assessed (12 of 19 animals examined), a discrete cluster of infected cells was consistently found in the diencephalon in the region of the subthalamic nucleus and the adjacent substantia nigra. A low-power view of such an area (Fig. 1A) illustrates the discrete localization of viral antigen bilaterally in an animal showing few antigen-positive cells in surrounding brain regions. The immunoreactivity in this patch consists of cellular profiles of variable size, cellular debris, and diffuse extracellular antigenic material. Much of the antigen was associated with vacuolation of the region (Fig. 1B). These antigen-positive regions were usually bilaterally symmetrical with discrete borders, and were evident in animals killed as early as 4 days after inoculation. The region involved contains many large neurons, and most of the identifiable antigen-containing cells appeared to be neurons. Many cells containing antigen were fragmented and unidentifiable as to cell type. Antigen also appeared to be present in the extracellular space, particularly in sections from severely affected animals. Cell loss, vacuolation, and gliosis (in animals with long intervals between inoculation and death) were seen in the subthalamic-nigral region in all moderately to severely affected animals (Fig. 1C). The cellular changes in this region were typical of those associated with coronavirus infection (*7*, *8*). Intracellular vacuolation was common, and many neurons appeared swollen, with pyknotic nuclei and loss of cytoplasmic detail. Larger vacuoles were packed within the region of cell loss, and vacuoles containing cellular fragments were commonly seen, suggesting that the larger vacuoles may have resulted from cell lysis. In moderately affected animals killed at intervals longer than 4 weeks after inoculation, the involved regions showed little viral antigen but were characterized by neuronal loss, persistent vacuolation, and gliosis.

The location of the intense patch of immunoreactivity varied little among animals. The subthalamic nucleus was most consistently involved, with the le-

Table 1. Clinical status of infected mice. Each letter [U (unaffected), M (moderately affected), and S (severely affected)] represents an individual animal examined histologically. Of 28 animals inoculated intracerebrally with 3000 plaque-forming units (PFU), 4 died, 8 were killed, and 16 survived. Of 30 animals given 4500 PFU, 8 died, 9 were killed, and 13 survived. Of 15 animals given 6000 PFU, 8 died and 7 were killed.

Weeks between inoculation and sacrifice	Dose of virus (PFU)		
	3000	4500	6000
1		MS	SSSS
2	UUM	MM	SS
3			M
4	M		
>4	MMMU		